

Review

A Comprehensive Review of Syngas Production, Fuel Properties, and Operational Parameters for Biomass Conversion

Saaida Khlifi ¹, Victor Pozzobon ^{2,*} and Marzouk Lajili ¹

¹ Laboratoire Etude des Milieux Ionisés et Réactifs (EMIR), Institut Préparatoire aux études d'Ingénieurs de Monastir (IPEIM), University of Monastir, Rue Ibn Eljazzar, Monastir 5019, Tunisia; marzouk.lajili@ipeim.rnu.tn

² Laboratoire de Génie des Procédés et Matériaux, Centre Européen de Biotechnologie et de Bioéconomie (CEBB), CentraleSupélec, Université Paris-Saclay, 3 rue des Rouges Terres, 51110 Pomacle, France

* Correspondence: victor.pozzobon@centralesupelec.fr

Abstract: This study aims to provide an overview of the growing need for renewable energy conversion and aligns with the broader context of environmentally friendly energy, specifically through producing syngas from biomass. Unlike natural gas, which is mainly composed of methane, syngas contains a mixture of combustible CO, H₂, and C_nH_m. Therefore, optimizing its production requires a thorough examination of various operational parameters such as the gasifying agent, the equivalence ratio, the biofuel type, and the state, particularly in densified forms like pellets or briquettes. As new biomass sources are continually discovered and tested, operational parameters are also constantly evaluated, and new techniques are continuously developed. Indeed, these techniques include different gasifier types and the use or non-use of catalysts during biofuel conversion. The present study focuses on these critical aspects to examine their effect on the efficiency of syngas production. It is worth mentioning that syngas is the primary gaseous product from gasification. Moreover, it is essential to note that the pyrolysis process (prior to gasification) can produce, in addition to tar and char, a mixture of gases. The common feature among these gases is their versatility in energy generation, heat production, and chemical synthesis. The analysis encompasses the resulting gas features, including the yield and composition, mainly through the hydrogen-to-carbon monoxide ratio and the carbon monoxide-to-carbon dioxide ratio, as well as the lower heating value and considerations of the tar yield.

Keywords: pyrolysis; gasification; syngas; waste; operating parameters

Citation: Khlifi, S.; Pozzobon, V.; Lajili, M. A Comprehensive Review of Syngas Production, Fuel Properties, and Operational Parameters for Biomass Conversion. *Energies* **2024**, *17*, 3646. <https://doi.org/10.3390/en17153646>

Academic Editor: Gartzen Lopez

Received: 16 June 2024

Revised: 5 July 2024

Accepted: 23 July 2024

Published: 24 July 2024



Copyright: © 2024 by the authors. Licensee MDPI, Basel, Switzerland. This article is an open access article distributed under the terms and conditions of the Creative Commons Attribution (CC BY) license (<https://creativecommons.org/licenses/by/4.0/>).

1. Introduction

Within Tunisia, natural gas takes the lead in energy consumption, accounting for 49.4% in 2021, closely followed by oil at 40.0% [1]. These fossil fuel sources find application not only in Tunisia but also globally, serving transportation and electricity generation needs. In the current era, fossil fuels present ecological challenges, as their use via combustion induces profound climate shifts stemming from the rising emissions of greenhouse gases (GHGs) [2,3]. Among these emissions, carbon dioxide (CO₂) stands as the primary contributor to GHGs. Statistics provided by the International Energy Agency indicate that over 82% of CO₂ emissions stem from the combustion of fossil fuels (coal, oil, and natural gas) [4]. Moreover, these fuels have high costs [5]. Together, these reasons are generating heightened interest in transitioning toward sustainable and eco-friendly energy sources, including solar energy (photovoltaic and thermal), biomass, hydrothermal, geothermal, and wind power. The notable advantage of utilizing lignocellulosic biomass or waste lies in the CO₂ emissions being perceived as recycled,

having been initially absorbed through photosynthesis during the plant growth phase [6]. Moreover, biomass is a unique source capable of yielding diverse fuel types: solid biofuels (chars), liquid biofuels (bio-oils and tars), and gas (or synthesis gas), respectively. These facts position biomass with substantial potential for further expansion in generating heat and/or electricity and transport fuels. Indeed, in 2020, global biomass and waste consumption amounted to 1394 million tons of oil equivalent (toe) [7], while in Tunisia, it reached 1066 thousand tons of oil equivalent [1]. These data correspond to approximately 9.83% and 10.2% of the total energy supply, respectively. It is worth noting that the term 'biomass' encompasses all thermally degradable organic materials derived from plants, animals, and human or industrial activities. Biomass is a renewable energy source derived from solar energy stored during the photosynthesis of plants. Due to its complex composition, including a variety of polymers, cellulose, hemicellulose, and lignin, it is called lignocellulosic biomass. Biomass can be converted into heat and/or electricity via combustion [8]. Also, other thermal processes enable us to produce alternative fuels like syngas, bio-oils, and chars through pyrolysis [9–16] and gasification [9,17]. The term syngas denotes a blend of gaseous components, potentially including mainly carbon monoxide (CO), hydrogen (H₂), methane (CH₄), carbon dioxide (CO₂), and steam (H₂O) [18–21]. In addition, trace amounts of other compounds like ethylene (C₂H₄) and ethane (C₂H₆) might also be present [22,23], along with acetylene (C₂H₂) [24,25] and propane (C₃H₈) [19,23]. Syngas also comprises impurities, including tars, sulfur compounds, hydrogen chloride (HCl), volatile particles, alkali compounds, and heavy metals depending on the biomass type [26]. The syngas produced can be used to power internal combustion engines, gas turbines, or combined heat and power systems to produce electricity and heat simultaneously. It is also a foundational element for manufacturing chemical compounds. However, several shortcomings still exist in the field: (1) The lower heating value (LHV) of syngas is still affected by steam water in the medium. (2) The yielded syngas is a mixture of reactive and non-reactive components, such as N₂. (3) To exploit the produced syngas, it is necessary to build a gas turbine plant or engine near the syngas production system. (4) The storage of produced syngas is still a challenge. (5) The production of syngas via electric furnaces entails high costs. As the LHV constitutes a crucial energetic parameter that has not been sufficiently studied, we conducted an investigation into the impact of the fuel properties (ultimate and proximate analyses) on this property (second section). Additionally, other parameters such as the gasifying agent, equivalence ratio, and the densified form of the biofuel are also of interest. Thus, we propose to address these aspects in the third section, which focuses on gasification. Finally, the present paper presents a critical overview of this domain of research based on several recent studies reported in the literature, in which researchers have emphasized the importance of achieving reliable, viable, and steady syngas production [17–20,22,24,25].

2. Pyrolytic Generation of Syngas

Syngas is the primary gaseous product resulting from thermal conversion processes, primarily produced through gasification [9,27]. It is important to note that the pyrolysis process can also produce a mixture of gases, commonly referred to as syngas, in addition to tar and char [9–16]. Demirbas and Arin [28] could be considered among the pioneers who first focused on biomass pyrolysis for syngas production. They noted that achieving high syngas yields during pyrolysis requires high temperatures, low heating rates, and extended gas residence times. In a similar vein, Kan et al. [29] explored various factors influencing syngas production. These factors encompass the biomass type, its inherent characteristics, the conversion methods, and thermal, physical, biological, and chemical pretreatments. The generation of syngas was historically confined to the thermal conversion of both fossil fuels (such as coal, char, natural gas, and petroleum) and lignocellulosic biomass [30]. Nevertheless, there is a substantial array of conventional waste products and hydrocarbon feedstocks suitable for this transformation. Biomass wastes can be categorized into three distinct groups based on their origins: agricultural

residues, which encompass a variety of materials such as date palm waste [14], walnut shells [31], almond shells [13], cotton stalks [32], wheat and barley straw [33], vine stems [34], oat straw [35], and rice husk [36]; waste from the olive oil industry, such as olive pomace waste [12], olive mill wastewater [37], and olive mill solid waste [38]; and agro-industrial waste, including tomato residues [39], grape marc [14], and spent coffee grounds [40]. Additionally, other bioresources include waste cooking oil [10], sewage sludge (municipal waste) [9], medical waste [41], and animal fatty wastes [11].

In Table 1, sixteen types of biomass are presented that were gathered from the literature, with a specific focus on biomass pyrolysis. All the selected pyrolysis tests were conducted under an inert atmosphere without the presence of catalysis. Ultimate and proximate analyses of published research concerning biomass are reported. In addition, Table 2 offers a comprehensive summary of published research on biomass used for syngas production, detailing the conditions of the syngas production (including the heating rate, temperature, and residence time) as well as the properties of the syngas (encompassing the proportion generated, composition, and corresponding lower heating value). In the undertaken research, the resulting gas primarily comprised CH₄, H₂, CO, CO₂, and other minor hydrocarbon trace components (C_nH_m) like C₂H₄ and C₂H₆. The lower heating value of the syngas was calculated using Equation (1) [42]:

$$LHV = (10.78H_2 + 12.63CO + 35.88CH_4 + 64.5C_nH_m) \times 0.0042 \quad (1)$$

The oxygen content was deduced by the following: $(100 - (C + H + M + \text{Ash})) = O$

Table 1. Ultimate and proximate analyses of the published research involving biomass.

| Sources | Ultimate Analysis | | | | | Proximate Analysis (wt%) | | | |
|---------------------------|-------------------|-------|-------|------|-------|--------------------------|-------------|-----------------|--------------|
| | C | H | O | N | S | Moisture Content | Ash Content | Volatile Matter | Fixed Carbon |
| Sewage sludge [9] | 48.21 | 8.17 | 10.15 | 1.71 | 0.96 | 9.49 | 30.80 | 58.81 | 0.90 |
| Olive pomace waste [12] | 47.34 | 6.6 | 41.31 | 2.73 | - | 3.44 | 2.02 | 73.22 | 21.32 |
| Date palm leaflets [14] | 43.14 | 7.49 | 37.59 | 0.2 | - | 8.50 | 11.58 | 72.28 | 7.64 |
| Date palm rachis [14] | 39.95 | 7.19 | 47.2 | 0.16 | - | 7.27 | 5.50 | 78.11 | 9.12 |
| Empty fruit bunch [14] | 43.49 | 7.51 | 44.61 | 0.19 | - | 7.68 | 4.20 | 81.20 | 6.92 |
| Date palm glaiich [14] | 43.65 | 7.59 | 46.2 | 0.16 | - | 6.58 | 2.40 | 83.84 | 7.18 |
| Walnut shells [31] | 49.26 | 5.38 | 43.9 | 0.28 | - | 7.85 | 1.18 | 80.21 | 10.76 |
| Bamboo [43] | 49.9 | 6.5 | 30.6 | 6.0 | 0.6 | 3.7 | 6.4 | 74.0 | 15.9 |
| <i>Pinus radiata</i> [44] | 47.8 | 7.6 | 44 | 0 | 0 | 10.6 | 0.6 | 70.7 | 18.1 |
| Cotton stalk [32] | 46.56 | 6.04 | 42.01 | 0.79 | - | 1.86 | 4.60 | 77.5 | 16.04 |
| Wheat straw [33] | 42.36 | 5.27 | 45.15 | 1.12 | >0.1 | 8.40 | 6.00 | 62.40 | 23.30 |
| Barley straw [33] | 42.44 | 5.25 | 44.73 | 1.18 | >0.1 | 8.60 | 6.30 | 62.10 | 23.10 |
| Medical waste [41] | 59.0 | 8.0 | 24.53 | 2.0 | 5.0 | 3.19 | 1.47 | 92.72 | 2.62 |
| Waste cooking oil [10] | 75.61 | 13.27 | 9.79 | 0.12 | 0.09 | - | 1.12 | - | - |
| Lamb fatty wastes [11] | 74.63 | 12.11 | 12.50 | 0.15 | 0.27 | - | 0.34 | - | - |
| Almond shells [13] | 45.64 | 6.19 | 45.43 | <0.5 | <0.05 | 7 | 2.71 | - | - |

In this section, we highlight the impact of proximate analysis on the lower heating value of syngas derived from biomass wastes using data from the literature (Figures 1–4). Each figure depicts two curves: the red curve represents samples pyrolyzed under identical conditions—heating rate of 15 °C/min, temperature of 500 °C, and residence time of 54 min—while the blue curve represents samples pyrolyzed under different but controlled conditions—heating rate of 20 °C/min, temperature of 600 °C, and residence time of 30 min.

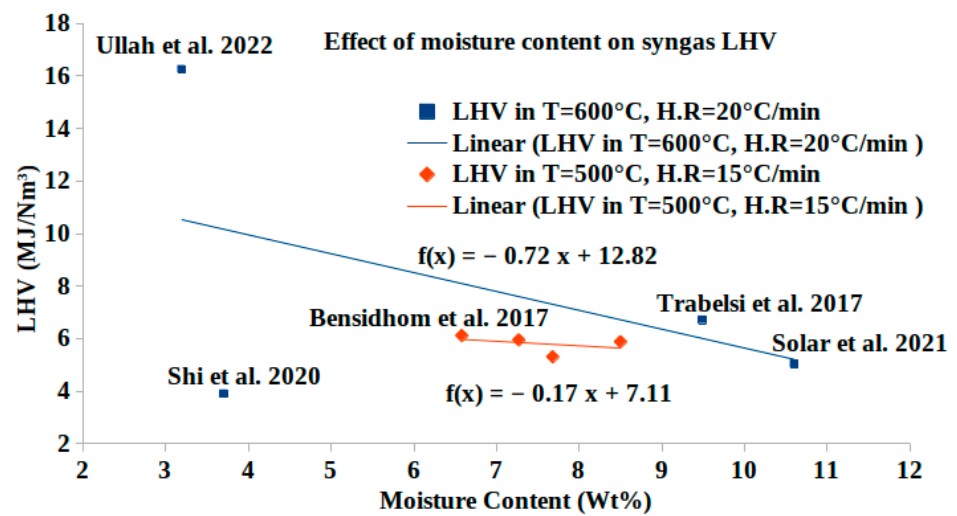


Figure 1. The effect of moisture content on syngas LHV [9,14,41,43,44].

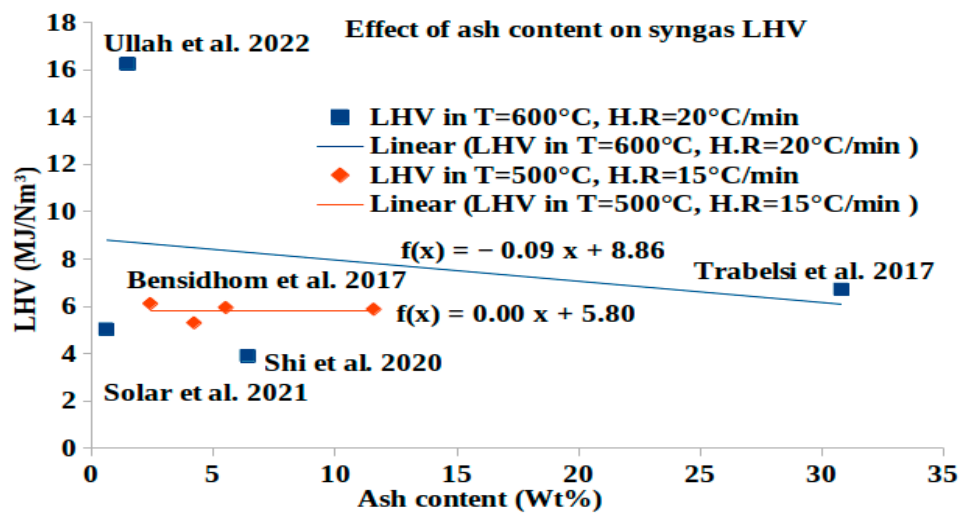


Figure 2. The effect of ash content on syngas LHV [9,14,41,43,44].

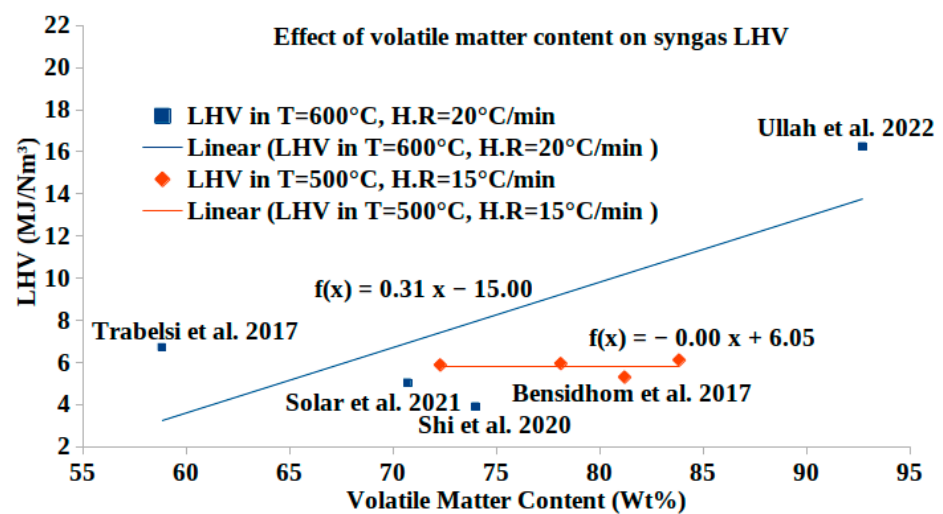


Figure 3. The effect of volatile content on syngas LHV [9,14,41,43,44].

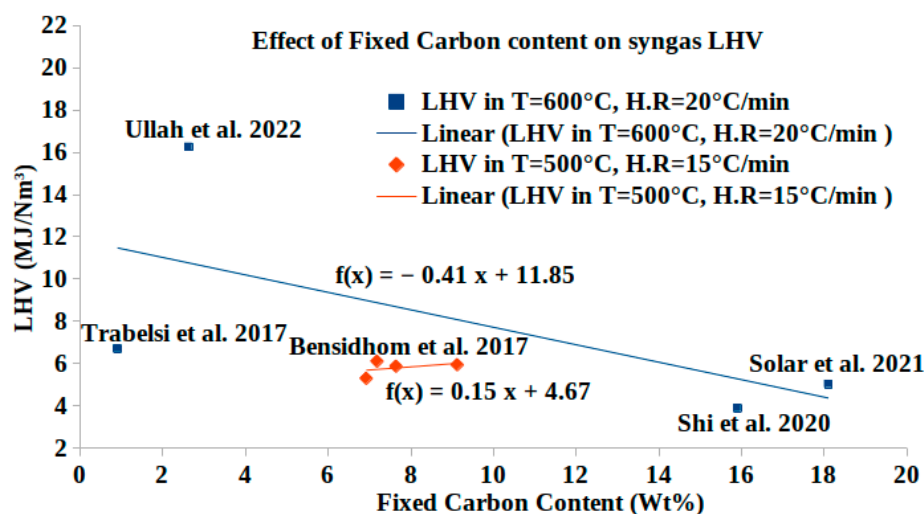


Figure 4. The effect of fixed carbon content on syngas LHV [9,14,41,43,44].

Figure 1 illustrates the impact of the moisture content on the syngas LHV. The figure reveals that in both cases (the blue and the red curves), within a moisture content range of from 3 to 11 wt%, the syngas LHV exhibited a significant decrease for the blue curve but a weak decrease for the red curve as the moisture content increased. These results are consistent with those found by [45–47]. According to Shehzad et al., the decrease in the syngas LHV was attributed to a reduction in the CO and CH₄ concentrations [45]. When comparing the syngas LHV of medical waste (16.25 MJ/Nm³) [41] with that of sewage sludge (6.716 MJ/Nm³) [9], we observed a higher CH₄ content in the medical waste (27.77 vol%) compared to the sewage sludge (17.16 vol%). Additionally, the CO content was also higher in the medical waste (11.27 vol%) compared to the sewage sludge (3.69 vol%).

Table 2. Summary of published research on biomass used for syngas production, detailing the conditions of syngas production (heating rate, temperature, and residence time) and the properties of the syngas (the proportion generated, composition, and corresponding lower heating value (LHV)). GY: gas yield. HR: heating rate.

| Source | Conditions of Syngas Production | | | Syngas | | | | | | |
|-------------------------|---------------------------------|------------------|----------------------|-----------|---------------------|-----------------|----------------|-------|-------------------------------|-------|
| | HR (°C/min) | Temperature (°C) | Residence Time (min) | GY (wt.%) | Composition (Vol %) | | | | LHV (MJ/Nm ³) | |
| | | | | | CH ₄ | CO ₂ | H ₂ | CO | C ₂ H ₆ | |
| Sewage sludge [9] | 20 | 600 | 30 | 21.77 | 17.16 | 2.31 | 74.69 | 3.69 | 2.17 | 6.716 |
| Olive pomace waste [12] | 15 | 600 | 40 | 37 | 10.54 | 0.34 | 52.08 | 35.65 | 1.39 | 6.213 |
| Date palm leaflets [14] | 15 | 500 | 54 | 46 | 7.14 | 0.26 | 30.36 | 61.65 | 0.6 | 5.88 |
| Date palm rachis [14] | 15 | 500 | 54 | 39 | 6.37 | 0.48 | 12.68 | 79.81 | 0.67 | 5.95 |
| Empty fruit bunch [14] | 15 | 500 | 54 | 40 | 5.09 | 0.11 | 70.89 | 23.63 | 0.28 | 5.305 |
| Date palm glaiich [14] | 15 | 500 | 54 | 43 | 9.92 | 0.33 | 39.53 | 49.45 | 0.77 | 6.116 |
| Walnut shells [31] | 5 | 600 | 120 | 15 | 13 | 29.84 | 16.66 | 40.48 | - | 4.861 |
| Walnut shells [31] | 5 | 500 | 100 | 8.9 | 8.56 | 37.8 | 15.77 | 39.77 | - | 4.113 |
| Bamboo [43] | 20 | 600 | 30 | - | 1.01 | 23.8 | 30.11 | 45.06 | - | 3.905 |
| Bamboo [43] | 20 | 700 | 35 | - | 4.64 | 16.96 | 43.73 | 34.64 | - | 4.51 |
| Pinus radiata [44] | 20 | 600 | 30 | 35.6 | 16.8 | 37.5 | 20.4 | 24.2 | 1.1 | 5.037 |
| Pinus radiata [44] | 17 | 500 | 30 | 26.4 | 13.8 | 48.5 | 20.1 | 14.0 | 3.6 | 4.7 |
| Cotton stalk [32] | 10 | 550 | 30 | 28.2 | 11.74 | 45.89 | 6.98 | 30.68 | 4.68 | 4.98 |
| wheat straw [33] | 7 | 600 | 90 | 20.16 | 8.75 | 51.55 | 9.54 | 28.12 | 2.03 | 3.79 |
| wheat straw [33] | 6 | 500 | 90 | 18.91 | 7.75 | 56.69 | 4.04 | 29.53 | 1.98 | 3.45 |

| | | | | | | | | | | |
|------------------------|----|-----|----|-------|-------|-------|-------|-------|------|-------|
| barley straw [33] | 7 | 600 | 90 | 19.1 | 10.33 | 49.1 | 10.55 | 27.84 | 2.18 | 4.10 |
| barley straw [33] | 6 | 500 | 90 | 20.26 | 8.86 | 55.06 | 3.91 | 29.76 | 2.41 | 3.74 |
| Medical waste [41] | 20 | 600 | 30 | 37.3 | 27.77 | 7.36 | 11.27 | 13.6 | 40.0 | 16.25 |
| Waste cooking oil [10] | 15 | 650 | - | 15.9 | 22.85 | 17.59 | 52.85 | 6.21 | 0.5 | 6.301 |
| Lamb fatty wastes [11] | 15 | 500 | 50 | 62 | - | - | - | - | - | - |
| Almond shells [13] | 10 | 537 | 50 | 47 | - | - | - | - | - | - |

Several research studies have found the following same results: as the moisture content increases, the production of hydrogen and carbon dioxide increases, while the production of CO and CH₄ decreases [45,47,48]. Dong et al. noted a decrease in energy conversion due to the increase in the moisture content [47]. This suggests that the gain in H₂ in the syngas could not fully compensate for the energy loss resulting from the reduced concentrations of CO, CH₄, and C_xH_y. When biomass waste is used for combustion applications, it is important to note that the ignition delay is prolonged with an increase in the moisture content. Wang et al. reported that under such conditions, the improvement in the fuel–air mixing quality due to water is weaker than its reducing effect on the local temperature [49]. Fraia et al. reported that increasing the pyrolysis temperature resulted in an increase in the CO and H₂ concentration whilst resulting in a decrease in the CO₂, CH₄, and C₂H₄ concentration [50]. Thus, the LHV increased more significantly with a rise in temperature from 500 °C to 600 °C and the heating rate from 15 °C/min to 20 °C/min, while a reduction in the residence time from 54 to 30 min resulted in a steeper slope of the trend line, which is the case with the blue curve.

Figure 2 illustrates the impact of the ash content on the lower heating value of syngas. The graph shows that as the ash content increases from 1 to 30 wt%, the LHV of the syngas generally decreases, with a trend line slope of $-0.09 \text{ MJ/Nm}^3/\text{wt}\%$. However, in the case of the red curve, where the ash content only ranges between 2 and 12 wt%, the ash content does not significantly impact the LHV, and the slope of the trend line in this range is nearly zero. The difference between the two curves' behavior is likely due to variations in the biomass source type [51]. Additionally, the presence of foreign material, which can occur when no cleaning process is followed, may have contributed to the differences observed [52]. When taking into consideration the blue curve, the syngas LHV of medical waste (16.25 MJ/Nm^3) is significantly higher than that of sewage sludge (6.716 MJ/Nm^3). This difference was attributed to the higher ash content in sewage sludge (30.8 wt%) compared to medical waste (1.47 wt%). Similar trends are observed when comparing the ash content of bamboo (6.4 wt%) with that of *Pinus radiata* (0.6 wt%); the LHV of bamboo (3.905 MJ/kg) is lower than that of *Pinus radiata* (5.037 MJ/kg). The high syngas yield from medical waste (37.3 wt%) compared to sewage sludge (21.77 wt%) contributes to its higher LHV, as a low ash content correlates with a higher syngas yield. Kardaś et al. found similar results, attributing high LHV values to low equivalence ratios, a low moisture content, a high volatile content, and a low fixed carbon content [53]. According to Bensidhom et al., a high syngas LHV may also be attributed to low weight percentages of cellulose, hemicellulose, and lignin [14]. Additionally, the ash content increases with the increase in the pyrolysis temperature [52]. This is probably due to the enhanced decomposition of lignocellulosic materials.

Figure 3 represents the effect of volatile matter on the syngas LHV. The red curve indicates that the LHV is not significantly affected by the volatile matter content, with a slope of nearly zero. This finding is expected due to the relationship between the ash and volatile matter contents. In contrast, the blue curves show a linear correlation between the LHV and volatile matter content, with a trend line slope of $0.31 \text{ MJ/Nm}^3/\text{wt}\%$, indicating that the LHV increases with increasing the volatile matter content [53].

Figure 4 illustrates the effect of the fixed carbon content on the lower heating value of syngas. The blue curve shows a decrease in syngas LHV with an increase in the fixed carbon content, while the red curve exhibits the opposite behavior, indicating that the LHV increases with increasing the fixed carbon content. This different behavior is likely

due to variations in the biomass source type [51]. The difference in the char content may also be influenced by a high lignin content, which leads to a higher char fraction [43]. Shi et al. found that increasing the pyrolysis temperature results in a decrease in the produced char and bio-oil contents, accompanied by an increase in the volatile matter content [43]. This finding is primarily due to the fact that higher temperatures provide more energy, facilitating the decomposition of biomass and enhancing its conversion to volatile matter.

3. Gasification for Syngas Production

It is essential to note that various types of gasification plants can be used in both research and industry. In addition, the choice of the crucial gasifier agent is essential during the thermal conversion in order to enhance the syngas yield, as discussed by Kan et al. [29]. Consequently, the question of the gasifying reactor type has already been addressed by numerous authors and will only be briefly reviewed here before focusing on key operating parameters. Samiran et al. conducted a comparative study on various types of gasifiers, revealing that achieving a carbon conversion rate exceeding 90% is feasible across most gasifier types [54]. They observed slight variations in the carbon conversion rate, primarily attributed to the difference in the selected operating parameters [54]. Moreover, as is reported in the literature, a range of gasifier reactor designs, including updraft fixed-bed, downdraft fixed-bed, bubbling fluidized-bed, circulating fluidized-bed, entrained-flow-bed, and twin fluidized-bed gasifiers, can be found. This categorization is based on the mixing mechanism between the reagents and the gasification agent, as discussed by Ruiz et al. [18]. Samiran et al. conducted an extensive evaluation of the characteristics, benefits, and drawbacks associated with different gasifier types, namely entrained-, fixed-, and fluidized-bed designs [54]. In scientific research, fixed-bed gasifiers are often preferred for several reasons; they enable the use of small quantities of raw material and entail shorter operating times [55]. Additionally, they remain a cost-effective technique for syngas production [54]. Havilah et al., on the other hand, opted for the downdraft fixed-bed gasifier type due to its suitability for studying pyrolysis and gasification reactions at the laboratory scale [56]. Furthermore, the study conducted by Ahmad et al. shows the impact of various factors, including the type of gasifier, temperature, biomass particle size, gasification agent, and bed material [57]. They highlighted that the temperature, equivalence ratio (ER), and use of a catalyst are the critical and determinant factors of efficient gasification from the point of view of efficiency and syngas quality. However, we restricted our study to only several parameters: the gasifying agent, the equivalence ratio, the biofuel type, and the state.

3.1. The Gasifying Agent

The gasification process can be carried out with various gasifying agents, which are widely discussed in the literature. These agents include air, CO₂, H₂O, and O₂, as was reported by [58,59]. Gallucci et al. investigated the impact of using air and steam as gasifying agents [60]. The authors observed that when air was used, the dominant component in the produced gas was nitrogen (inert gas making up 50% of the total volume), while methane and hydrogen together constituted approximately 13%. The generated CO and CO₂ accounted for 25.3% and 11.6%, respectively. Conversely, using steam as a gasifying agent resulted in syngas with higher concentrations of H₂ (35.5%), CO (31.8%), CO₂ (18.1%), and CH₄ (14.6%). This highlights that gasification with air leads to a gas product diluted with nitrogen. Hence, they observed that when operating with air, the LHV was lower (9.304 MJ/Nm³) compared to using steam (13.1 MJ/Nm³), which is a consistent result with the literature [59]. Furthermore, a comparative study was conducted regarding the LHV using CO₂ and oxygen as gasifying agents. It was observed that syngas obtained from the thermal conversion of biomass using CO₂ exhibited a lower LHV compared to syngas produced when oxygen was used, as reported by Fiore et al. [59]. In addition, Pinto et al. undertook a comparative analysis of gasification processes using oxygen and air as gasifying agents [61]. They presented the gas composition on a

dry, inert-free basis when air was employed as the gasifying agent. However, they did not observe any significant alterations in either the gas composition or LHV [61]. Indeed, during the thermal conversion of the biomass using steam, there was an improvement in hydrogen (H₂) production. Ceronea et al. [23] noticed an increase in H₂ production from 23.2 g/kg to 37.5 g/kg for gasification with air (A(21)) and air/steam (AS) ratios at specific conditions (21, 16). They also observed an increase in the H₂/CO ratio from 0.46 to 0.77 when operating with air and air/steam at different conditions (19, 11). However, the presence of steam had an effect on tar production. According to the results found by Ceronea et al., tar production increased from 137 g/kg to 163 g/kg during air (A) and air/steam (AS) gasification tests at specific conditions (21, 16) [23]. Steam primarily contributed to an increase in the LHV. Moreover, the use of an oxygen-and-steam mixture with an equivalence ratio of 0.2 favored the formation of sulfur compounds such as hydrogen sulfide (H₂S) and ammonia (NH₃), as reported by Pinto et al. [61]. Additionally, the yields of carbon dioxide (CO₂) and hydrogen (H₂) were found to increase compared to the results obtained using air and steam at various equivalence ratios (ER = 0.2, 0.3). These two gas compounds increased with higher oxygen contents when operating with air enriched by oxygen. In such conditions, two key equations, the water–gas shift and the oxidation equations, should be taken into account [62].



Nonetheless, CH₄, CO, and hydrocarbons (C_nH_m) exhibited a decline as the oxygen content increased [61]. On the contrary, CH₄ and C_nH_m showed higher levels when the gasification process was carried out using air and steam at an ER of 0.2, indicating that methanation (Equation (4)) and H₂/steam reforming (Equation (5)) took place. On the other hand, the CO yield increased when air was employed as a gasifying agent compared to scenarios involving air and steam, oxygen and steam, or steam alone, indicating a predominance of the partial oxidation reaction (Equation (6)).



Augmenting the quantity of the supplied CO₂ led to an elevation in the carbon monoxide (CO) while simultaneously leading to a reduction in the carbon dioxide (CO₂) present in the generated gas. This phenomenon can be attributed to the involvement of CO₂ in stimulating the Boudouard reaction (Equation (7)). When the gasification process was conducted with the presence of CO₂, there was an overall increase in the total gas yield, accompanied by a reduction in the formation of tar and ammonia (NH₃), as observed in the study of Pinto et al. [61]:



3.2. Equivalence Ratio

The equivalence ratio is determined by dividing the real oxygen-to-fuel ratio by the stoichiometric oxygen-to-fuel ratio required for complete combustion. Table 3 illustrates the effect of gasifier technology (GT), equivalence ratio (ER), and gasifying agent (GA) on the lower heating value (LHV), hydrogen-to-carbon monoxide ratio (HCMR), carbon monoxide-to-carbon dioxide ratio (CMCDR), tar yield (TY), and gas yield (GY). In the study conducted by Lv et al. [63], pine sawdust gasification was carried out within a fluidized-bed gasifier using an air–steam mixture, with dolomite and nickel serving as catalysts. The authors observed that when elevating the ER from 0.25 to 0.3, an increase in

the hydrogen-to-carbon monoxide ratio (HCMR) from 1.46 to 1.54 accompanied by a decrease in the carbon monoxide-to-carbon dioxide ratio (CMCDR) from 0.99 to 0.9 occurred. Furthermore, the tar yield exhibited a reduction from 19.05 to 13.85%, while the gas yield experienced a slight increase from 1.54 to 1.56. Moreover, Zheng et al. concluded that when raising the ER from 0.2 to 0.5, the proportions of produced H₂, CO, and CH₄, dropped from 16.7% to 3.17%, 23.9% to 6.34%, and 2.88% to 0.3%, respectively [24]. Conversely, there was an increase in CO₂ from 55.79% to 88.8%. Consequently, the LHV of the syngas decreased from 5.97 MJ/Nm³ to 1.30 MJ/Nm³. In the same context, Khezri et al. [64] observed a similar trend to that reported by Zheng et al. [24] when the ER increased from 0.2 to 0.4. Indeed, they noted a decrease in H₂ from 19.8% to 9.68%, CO from 5.81% to 2.67%, and CH₄ from 8.94% to 3.13%, whereas CO₂ exhibited a slight decrease from 11.53% to 10.51%, whereas the gas yield increased from 1.94 to 2.45 Nm³/kg, in agreement with Lv et al.'s observation [63]. Moreover, the carbon conversion efficiency (CCE) declined from 61.5% to 53.15%, mirroring a decrease in the cold gas efficiency (CGE) from 78.9% to 43.2% within the same ER range [64].

Katsaros et al. noted that as the ER increased from 0.17 to 0.21, there was a clear uptick in the gas yield, rising from 1.221 to 1.247 Nm³/kg biomass, while tar production dropped from 4.87 to 4.25 g/kg biomass [65]. These findings are consistent with the observations of Lv et al. [63], indicating a reliable trend. Additionally, the LHV values showed a marginal reduction from 4.22 to 4.20 MJ/Nm³, confirming the results reported by Zheng et al. [24]. Regarding poultry litter, the CCE showed a minor decrease from 85.5% to 85.1%, with a corresponding decrease in the CGE from 61% to 58% [65]. These trends closely mirror the results reported by [64]. For beech wood, the CGE declined from 62.93% to 61.96%, while the CCE experienced an increase from 82.76% to 91.6% [65].

Furthermore, when the ER increased from 0.18 to 0.27, the tar yield decreased from 7.52 to 6.72 g/kg biomass, aligning with the results reported by [63]. Simultaneously, the gas yield increased from 0.86 to 0.976 Nm³/kg biomass, which is consistent with the findings of both teams [63,64]. Indeed, the LHV exhibited a decrease from 4.96 to 4.82 MJ/Nm³, which is in line with the results reported by [24]. Moreover, Zhao et al. noticed that as the ER increased from 0.23 to 0.32, there was a reduction in the tar yield from 6.85 to 4.96 g/Nm³ [66], which was consistent with reported findings [63,65]. The LHV decreased from 4.23 to 3.63 MJ/Nm³, in alignment with the outcomes reported [24,65]. Additionally, the CCE increased from 47.25% to 62.75%, while the CGE increased from 29.96% to 37.44%. It is noteworthy that these results contradict the findings of [64]. In their investigation, Zhao et al. focused on the influence of the ER on temperature and observed that when the ER increased from 0.23 to 0.32, the temperature rose from 679 °C to 795 °C [66]. Also, Jayathilake et al. [67] observed that the cold gas efficiency initially increased from 36.94% to 55.79% as the ER rose from 0.2 to 0.35. However, it then decreased from 55.79% to 52.02% as the ER further increased from 0.35 to 0.5. Additionally, the gas yield exhibited an initial increase from 1.76 to 2.6 and then decreased to 2.56. Similarly, the LHV initially rose from 3.72 MJ/Nm³ to 3.82 MJ/Nm³ and subsequently decreased to 3.61 MJ/Nm³. The HCMR showed a consistent increase from 0.47 to 0.31, while the CMCDR initially decreased from 1.63 to 1.38, with the ER going from 0.2 to 0.35, but it then decreased from 1.38 to 1.27 as the ER increased from 0.35 to 0.5. In addition, Atnaw et al. [68] observed that as the ER increased from 0.37 to 0.49, the LHV decreased from 4.83 MJ/Nm³ to 3.32 MJ/Nm³, corroborating the findings reported by [24,65,66]. Similarly, in line with results from [63,65,66,68,69], the HCMR increased from 0.57 to 0.65 [68]. Furthermore, consistent with the outcomes observed by [63,65–69], the CMCDR decreased from 1.81 to 0.88 [68]. According to a study by Skoulou [69], there was an increase in the LHV from 10.38 MJ/Nm³ to 10.5 MJ/Nm³ as the ER increased from 0.14 to 0.21. However, the LHV subsequently decreased from 10.5 MJ/Nm³ to 8.75 MJ/Nm³ as the ER further increased from 0.21 to 0.41. A similar trend was reported in [24,65,66,68]. Indeed, the HCMR initially increased from 1.53 to 1.69 as the ER rose and then decreased back to 1.53.

Similarly, the CMCDR exhibited a decrease from 0.51 to 0.48 and then to 0.42 as the ER changed, respectively, from 0.14 to 0.21 to 0.41.

Table 3. Effect of gasifier technology (GT), equivalence ratio (ER), and gasifying agent (GA) on lower heating value (LHV), hydrogen-to-carbon monoxide ratio (HCMR), carbon monoxide-to-carbon dioxide ratio (CMCDR), tar yield (TY), and gas yield (GY).

| Biomass | GT | T (°C) | GA | Catalyst | ER | LHV | H ₂ /CO | CO/CO ₂ | TY | GY |
|--------------------------------|------------------------------|--------|-----------------------------|--|-----------|-------|--------------------|--------------------|-------|-------|
| Pine sawdust [63] | fluidized-bed | 800 | air–steam mixture | dolomite and nickel | 0.3 | - | 1.54 | 0.9 | 13.85 | 1.56 |
| Pine sawdust [63] | fluidized-bed | 800 | air–steam mixture | dolomite and nickel | 0.25 | - | 1.46 | 0.99 | 19.05 | 1.54 |
| Bamboo [24] | updraft fixed-bed | 800 | steam | no | 0.2 | 6.2 | 0.71 | 0.43 | - | - |
| Wood residue [70] | fluidized-bed | 823 | mixture of oxygen and steam | Ni/Al ₂ O ₃ (20 wt%) | 0.17 | - | 1.22 | 0.48 | - | 1.31 |
| Palletized Napier grass [64] | fluidized-bed gasifier | 800 | air | no | 0.2 | - | 3.44 | 0.5 | - | 1.93 |
| White pine [71] | fluidized-bed | 750 | air–steam | no | 0.3 | 4.65 | 3.9 | 0.18 | - | 2.18 |
| Citrus peels [71] | fluidized-bed | 750 | air–steam | no | 0.3 | 3.88 | 2.4 | 0.5 | - | 2.38 |
| <i>Posidonia Oceanica</i> [71] | fluidized-bed | 750 | air–steam | no | 0.3 | 2.67 | 6.0 | 0.2 | - | 2.7 |
| Poultry litter [65] | bubbling fluidized-bed | 750 | air | no | 0.17 | 4.22 | 0.9 | 1.1 | 4.87 | 1.22 |
| Poultry litter [65] | | | | | 0.21 | 4.2 | 0.89 | 0.98 | 4.25 | 1.247 |
| Beech wood [65] | bubbling fluidized-bed | 750 | air | no | 0.18 | 4.96 | 0.5 | 1.14 | 7.52 | 0.86 |
| Beech wood [65] | bubbling fluidized-bed | 750 | air | no | 0.22 5 | 4.86 | 0.55 | 1.0 | 7.44 | 0.948 |
| Beech wood [65] | bubbling fluidized-bed | 750 | air | no | 0.27 | 4.82 | 0.46 | 0.95 | 6.72 | 0.976 |
| Rice husks [66] | autothermal cyclone gasifier | 853 | air | no | 0.23 | 4.23 | 0.12 | 1.45 | 6.85 | - |
| Rice husks [66] | autothermal cyclone gasifier | 888 | air | no | 0.29 | 3.99 | 0.1438 | 1.28 | 5.07 | - |
| Rice husks [66] | autothermal cyclone | 908 | air | no | 0.32 | 3.63 | 0.1435 | 1.14 | 4.96 | - |
| Birchwood [67] | fixed-bed downdraft | - | air | no | 0.2 | 3.72 | 0.47 | 1.63 | - | 1.76 |
| Birchwood [67] | fixed-bed downdraft | - | air | no | 0.35 | 3.82 | 0.31 | 1.38 | - | 2.6 |
| Birchwood [67] | fixed-bed downdraft | - | air | no | 0.5 | 3.61 | 0.27 | 1.27 | - | 2.56 |
| Oil palm fronds [68] | downdraft gasifier | | air | no | 0.37 | 4.83 | 0.57 | 1.81 | - | - |
| Olive kernel [69] | downdraft fixed-bed | - | air | no | 0.14 | 10.38 | 1.53 | 0.51 | - | - |
| Olive kernel [69] | downdraft fixed-bed | - | air | no | 0.21 | 10.5 | 1.69 | 0.48 | - | - |
| Olive kernel [69] | downdraft fixed-bed | - | air | no | 0.41 | 8.75 | 1.53 | 0.42 | - | - |

| | | | | | | | | | | |
|--------------------------|---------------------|---|-----|----|------|-------|------|------|---|---|
| Olive tree cuttings [69] | downdraft fixed-bed | - | air | no | 0.14 | 11.32 | 1.38 | 0.45 | - | - |
| Olive tree cuttings [69] | downdraft fixed-bed | - | air | no | 0.21 | 10.38 | 1.71 | 0.41 | - | - |
| Olive tree cuttings [69] | downdraft fixed-bed | - | air | no | 0.41 | 8.06 | 1.53 | 0.25 | - | - |

Meng et al. [72] conducted a gasification investigation involving corn stalk briquettes, wherein they analyzed various gaseous compounds, including H₂, CO, CH₄, CO₂, N₂, O₂, C₂H₄, and C₂H₆. They observed that an increase in the ER from 0.31 to 0.41 resulted in a substantial rise in CO₂ production from 9.2% to 29.7%. Conversely, there was a decrease in H₂ from 35% to 27% and a decrease in CO from 53% to 40.78%. The CH₄ content decreased 1.67% to 1.04%. Moreover, the lower heating value decreased from 11.675 to 8.562 MJ/Nm³ as the ER increased from 0.31 to 0.40. Comparatively, the LHV of the gas produced from corn stalk briquettes (11.217 MJ/Nm³) exceeded that of pine wood blocks (10.453 MJ/Nm³) at an ER of 0.32. In terms of the gas yield, pine wood blocks outperformed corn stalk briquettes, with a gas yield of 91% versus 88% at an ER of 0.31. The gas yield substantially increased from 88% to 96% with an increase in the ER from 0.31 to 0.40. The carbon conversion efficiency also exhibited an upward trend, increasing from 71.53% to 81% as the ER increased from 0.31 to 0.40. Notably, the carbon conversion efficiency for corn stalk briquettes (71.53%) was lower than that for pine wood blocks (76.8%) at an ER of 0.31. Lastly, the tar yield for corn stalk briquettes was higher at 15.8% compared to pine wood blocks at 14.14%. However, the tar yield decreased as the ER increased from 0.31 to 0.40, reaching 8.55%.

The general trend is that an increase in ER can enhance the gas yield and reduce the tar yield, and it also reduces the quality (LHV) of the syngas and decreases overall efficiencies (CCE and CGE).

3.3. The Effect of the Form of the Biomass

The original biomass can primarily be compressed into pellets [73,74] or briquettes [75,76], known as renewable densified fuels. Table 4 presents a list of densified biomasses, specifically pellets and briquettes, as well as the diameter and length measurements for each sample from various sources according to different references. Both pellets and briquettes typically exhibit a cylindrical shape. The primary distinction between pellets and briquettes lies in their size dimensions. Pellets generally have diameters ranging from 6 to 10 mm and lengths between 10 and 40 mm. Conversely, briquettes tend to have diameters ranging from 20 to 60 mm and lengths between 30 and 90 mm.

Table 4. A list of densified biomasses, specifically pellets and briquettes, as well as the diameter and length measurements for each sample from various sources according to different references.

| Densified Biomass | Diameter (mm) | Length (mm) | References |
|--|---------------|-------------|------------|
| Wood pellets | 6 | 30–40 | [77] |
| Grass pellets | 7 | 30–40 | [77] |
| Wood pellets | 7 | 20 | [21] |
| Pellets from spruce wood, hay, and wheat straw | 8 | - | [78] |
| Wood, bark, and sunflower husk pellets | 8–10 | - | [79] |
| Wood pellets | 6 | 10–25 | [80] |
| Miscanthus briquettes | 20 | 30 | [81] |
| Soybean briquettes | 60 | 60–85 | [76] |
| Pigeon pea briquettes | 30 | 65–90 | [76] |
| Soybean–pigeon pea mixture briquettes | 60 | 65–80 | [76] |
| Sewage sludge briquettes | 45 | 40–50 | [82] |

| | | | |
|--|----|-------|------|
| Rice straw briquettes (binder: cotton stalk) | - | 45–50 | [83] |
| Olive pits briquettes | 50 | 70 | [84] |
| Sawdust briquette | 95 | 30–35 | [85] |

3.3.1. The Gasification of the Pellets

Table 5 provides information from the literature on the densified biomass, gasifier type, operating temperature, gasifier agent, ER, LHV, HCMR, and CMCDR for the generated gas. In the first step, the classification of the densified pellets is based on their LHV. Considering the research conducted by Niels et al. [86], who carried out gasification in an allothermal gasifier (heating of biomass from an external source) with a steam atmosphere using 800 g of olivine (Mg^{2+} , Fe^{2+}) $_2\text{SiO}_4$ as a catalyst, the LHV of wood pellets (8.0 MJ/m³) was higher than that of straw pellets (7.9 MJ/m³). Niels et al. [86] performed gas analysis for CO₂, H₂, CO, CH₄, C₂H₄, and C₃H₈ for reactor temperatures of 790 °C and 824 °C, respectively. They observed that the HCMR was increased for wood pellets (0.83) compared to straw pellets (0.79). Similarly, the CMCDR was also higher for wood pellets (0.6) compared to straw pellets (0.5). In the case of tar production, the wood pellets yielded less tar (0.1 g tar/g fuel) than straw pellets (0.165 g tar/g fuel) [86].

Table 5. The effect of biomass densified into pellets, including the gasifier type (GT), the temperature (T), the gasifying agent (GA), and the equivalence ratio (ER) on the lower heating value (LHV), hydrogen-to-carbon monoxide ratio (HCMR), carbon monoxide-to-carbon dioxide ratio (CMCDR), the carbon conversion efficiency (CCE), and cold gas efficiency (CGE) of the produced gas, extracted from the literature.

| Biomass | GT | T (°C) | GA | Catalyst | ER | LHV | H ₂ /CO | CO/CO ₂ | CCE (%) | CGE (%) |
|---------------------------------------|------------------------|--------|-------|--|-------|------|--------------------|--------------------|---------|---------|
| Wood–coconut fiber pellets [87] | downdraft gasifier | 900 | air | no | 0.32 | 3.58 | 7.1 | 0.16 | - | - |
| Rice husk pellets [87] | downdraft gasifier | 700 | air | no | 0.32 | 2.8 | 3.7 | 0.32 | - | - |
| Wood pellets [21] | downdraft | 877 | air | no | 0.278 | - | 0.84 | 3.76 | - | 87.6 |
| Spruce wood pellets [78] | fix-bed gasifier | 800 | air | no | n.d | 5.78 | 0.41 | 2.65 | - | - |
| Hay pellets [78] | fix-bed gasifier | 800 | air | no | n.d | 4.48 | 0.44 | 1.37 | - | - |
| Wheat straw pellets [78] | fix-bed gasifier | 800 | air | no | n.d | 3.93 | 0.44 | 1.32 | - | - |
| Wood pellets [88] | dual fluidized-bed | 800 | steam | no | n.d | - | 1.9 | 0.807 | - | - |
| Pine waste pellets (vol. %, dry) [89] | bubbling fluidized-bed | 800 | air | no | 0.25 | 5.4 | 0.37 | 1.25 | 96.1 | 72.9 |
| Straw pellets [86] | allothermal gasifier | 824 | steam | (Mg^{2+} , Fe^{2+}) $_2\text{SiO}_4$ | n.d | 7.9 | 0.79 | 0.5 | - | - |
| Wood pellets [86] | allothermal gasifier | 790 | steam | (Mg^{2+} , Fe^{2+}) $_2\text{SiO}_4$ | n.d | 8.0 | 0.83 | 0.6 | - | - |

Moreover, Mikeska et al. [78] conducted a study on the gasification of spruce wood, hay, and wheat straw pellets, analyzing various gas compounds, including O₂, CO₂, H₂, CO, CH₄, and N₂. The LHV of the spruce wood pellets (5.78 MJ/Nm³) was higher than that of the hay pellets (4.48 MJ/Nm³), which, in turn, was higher than that of the wheat straw pellets (3.93 MJ/Nm³). However, the HCMR of the spruce wood pellets (0.41) exhibited a lower value compared to both the hay and wheat straw pellets, which shared the same value of 0.44. Meanwhile, the CMCDR decreased from 2.65 for the spruce wood pellets to 1.37 for the hay pellets and further to 1.32 for the wheat straw pellets. The tar yield before cleaning was 7.43 g/Nm³ for spruce wood, 6.99 g/Nm³ for hay, and 6.76 g/Nm³ for wheat straw. Additionally, the nitrogen (N₂) content and oxygen (O₂) content fell within the

respective ranges of 49–58 wt% and 0.4–0.9 wt%. Also, in a distinct investigation, Wiyono et al. [87] conducted experiments to scrutinize the gasification process of wood–coconut fiber (WCF) and rice husk (RH) pellets. They conducted analyses on the concentrations of N_2 , H_2 , CO , CO_2 , and CH_4 within the resultant gases. These experiments were carried out using a downdraft gasifier operating under an air atmosphere. Under the same equivalence ratio ($ER = 0.32$), it was observed that the LHV was greater for the WCF pellets compared to the RH pellets, measuring 3.58 MJ/Nm^3 and 2.8 MJ/Nm^3 , respectively. Similarly, the HCMR was higher for the WCF pellets (7.1) than for the RH pellets (3.7). Conversely, the CMCDR was lower for the WCF pellets (0.16) compared to the RH pellets (0.32). Additionally, the reactor temperature was higher when using the WCF pellets than when using the RH pellets. The authors noted that the ash content was slightly higher for the WCF pellets (8.64%) compared to the RH pellets (8.61%). This ash primarily consisted of inorganic impurities, with NH_3 , HCN , H_2S , and fine dust being the primary constituents [87]. Aydin et al. [75] realized a comparative analysis involving pinecone particles and wood pellets. Their experimental measurements focused on the concentrations of various gaseous compounds, including CO , CO_2 , CH_4 , H_2 , and O_2 . Under an identical temperature and gasifier agent, it was observed that the wood pellets exhibited a lower HCMR of 0.8, whereas the pinecone particles presented a higher HCMR of 0.9. Conversely, the CMCDR was higher for the wood pellets (3.6) compared to the pinecone particles (2.46). Notably, the ER was slightly higher for the pinecone particles (0.27) compared to the ER of the wood pellets (0.26). Schweitzer et al. [88] conducted research on the gasification of wood pellets within a dual fluidized-bed system. They carried out analyses on the gas composition, including CO , CO_2 , CH_4 , H_2 , and non-condensable hydrocarbons (C_2 – C_4). Silica sand was used as the bed material in their experiments. The wood pellets used in their study exhibited a gas composition similar to that of sewage sludge and manure. It is worth noting that the concentration of inorganic impurities such as tar, NH_3 , H_2S , and Cl in the wood pellets was found to be lower when compared to sewage sludge and manure [88]. Nobre et al. [89] conducted an experimental investigation on the gasification of pine waste pellets within an air atmosphere under a temperature of $800 \text{ }^\circ\text{C}$ using a bubbling fluidized-bed reactor. The resulting gas mixture consisted of CO , CO_2 , CH_4 , H_2 , C_2H_4 , C_2H_6 , benzene, and toluene. The LHV of the pine waste pellets was 5.4 MJ/Nm^3 , with an HCMR of 0.37 and a CMCDR of 1.25. Similarly, spruce wood pellets, with an LHV of 5.78 MJ/Nm^3 , were gasified in a fixed-bed gasifier at a temperature of $800 \text{ }^\circ\text{C}$ under an air atmosphere. In this case, the HCMR and CMCDR were 0.41 and 2.65, respectively. In the second step, the classification of the densified pellets was based on their HCR. We found that the wood–coconut fiber pellets (7.1) ranked first, followed by the rice husk pellets (3.7) [87]. This gasification was realized in a downdraft gasifier, where air was the oxidizer. The temperature reached $900 \text{ }^\circ\text{C}$, and the ER was 0.32. The CMCDR values were 0.16 and 0.32, respectively. We found that the wood pellets ranked third (1.9) [88], where the gasification test was realized in a dual fluidized-bed gasifier. The temperature reached $800 \text{ }^\circ\text{C}$, and steam was the oxidizing agent. The CMCDR was 0.807.

3.3.2. The Gasification of the Briquettes

Table 6 provides a compilation of data from various literature sources, displaying examples of biomass transformed into briquettes. The table includes information on the type of gasifier, operating temperature, gasifying agent, ER, LHV, HCMR, CMCDR, and CCE for the resulting gas.

The reported results vary due to differences in the reactor types, gasifying agents, and ER values employed in the experiments. Additionally, the composition of the analyzed gases differed depending on the type of biomass briquette used.

For instance, Dogru analyzed gases from olive pits briquettes and identified H_2 , O_2 , N_2 , CH_4 , CO , CO_2 , C_2H_2 , and C_2H_6 [84]. Arjarn examined sewage sludge briquettes and identified CO , H_2 , CH_4 , N_2 , O_2 , and CO_2 [82]. Meng et al. investigated corn stalk briquettes and detected CO , H_2 , CH_4 , CO_2 , and C_2H_4 [72]. Raj et al. gasified sawdust briquettes,

observing CH₄, CO, CO₂, H₂, and N₂ [85]. Shaharin et al. studied oil palm fronds briquettes in an updraft gasifier, finding CO, CO₂, H₂, and CH₄ [90].

Comparing the results in the table, it is evident that corn stalk briquettes exhibited the highest LHV at 11.2 MJ/Nm³. This gasification process occurred in a fixed-bed gasifier under an oxygen atmosphere at a reactor temperature of 923 °C. Olive pit briquettes followed, with an LHV of 5.04 MJ/Nm³, gasified in a downdraft fixed-bed gasifier under an air atmosphere with a reactor temperature exceeding 1000 °C. Sewage sludge briquettes ranked third, with proper gasification achieved in a downdraft gasifier under an air atmosphere. In this case, the HCMR was inversely proportional to the LHV, with corn stalk briquettes having the lowest HCMR (0.7), followed by olive pits briquettes (0.78) and then sewage sludge briquettes (1.2).

Regarding the CMCDR, it followed a similar trend as the LHV, with corn stalk briquettes having the highest value (4.07), followed by sewage sludge briquettes (1.1) and then olive pits briquettes (1.27). Olive pits briquettes achieved a higher CCE (>97%) compared to corn stalk briquettes (73.93%). This suggests that as LHV increases, the CCE tends to decrease.

Overall, while both pellets and briquettes are densified forms of biomass, they exhibit differences in their lower heating values, hydrogen-to-carbon ratios, carbon monoxide-to-carbon dioxide ratios, and gasification conditions. These differences can impact their suitability for various applications, such as energy production and gasification processes.

Table 6. The effect of biomass densified into briquettes, including the gasifier type (GT), the temperature (T), the gasifying agent (GA), and the equivalence ratio (ER) on the lower heating value (LHV), hydrogen-to-carbon monoxide ratio (HCMR), carbon monoxide-to-carbon dioxide ratio (CMCDR), the carbon conversion efficiency (CCE), cold gas efficiency (CGE), the tar yield (TY), and gas yield (GY) of the produced gas, extracted from the literature.

| Biomass | GT | T (°C) | GA | Catalyst | ER | LHV | H ₂ /CO | CO/CO ₂ | CCE (%) | CGE (%) | TY (g/Nm ³) | GY (Nm ³ /kg) |
|-----------------------------------|---------------------|---------|-------------|----------|------|------|--------------------|--------------------|---------|---------|-------------------------|--------------------------|
| Sewage sludge briquettes [82] | downdraft gasifier | 780 | air | no | 0.24 | 4.87 | 1.2 | 1.1 | - | - | 0.07678 | 1.47 |
| Olive pits briquettes [84] | downdraft fixed-bed | >1000 | air | no | - | 5.04 | 0.78 | 1.27 | >97 | 68.21 | 0.796 | - |
| Sawdust briquettes [85] | downdraft gasifier | 800–900 | air | no | - | 3.21 | 0.72 | 1.57 | - | - | 4 | - |
| Corn stalk briquettes [72] | fixed-bed gasifier | 923 | oxy- gen | no | 0.32 | 11.2 | 0.7 | 4.07 | 73.93 | - | - | - |
| Fronds briquettes (oil palm) [90] | updraft gasifier | 734 | air | no | - | - | 0.25 | 1 | - | - | - | - |

4. Conclusions

This paper provides valuable insights into the factors influencing the syngas lower heating value in biomass pyrolysis processes, thereby contributing to the optimization of bioenergy production from a variety of biomass sources. They underscore the importance of selecting appropriate gasifying agents and understanding their effects on the gas composition, LHV, and byproduct formation in biomass gasification processes, thus promoting the optimization of bioenergy production and enhancing environmental sustainability.

Furthermore, these studies emphasize the significance of optimizing the equivalence ratio to achieve the desired gasification performance. They shed light on the diverse effects of equivalence ratio variations on the gasification parameters across different feedstocks.

Moreover, the importance of feedstock selection and the gasification parameters in achieving optimal gasification performance is highlighted, with variations in the LHV,

hydrogen-to-carbon monoxide ratio, and carbon monoxide-to-carbon dioxide ratio influencing the efficiency and characteristics of the generated gas.

In conclusion, these findings underscore the necessity of considering both biomass type and gasification parameters to optimize gasification processes for efficient energy conversion.

In the future, research should work on the separation of the syngas components using techniques like chemical looping chemistry. Moreover, the effect of mineral catalysts is highly recommended in order to increase the syngas yield, especially as some minerals are known by their inhibitor effects and others by their activator effects. In addition, it is time to extend studies from small-scale laboratory studies to industrial-scale ones.

Author Contributions: Conceptualization, S.K. and M.L.; validation, V.P. and M.L.; formal analysis, S.K. and M.L.; investigation, S.K.; writing—original draft preparation, S.K.; writing—review and editing, V.P. and M.L.; supervision, M.L. All authors have read and agreed to the published version of the manuscript.

Funding: Communauté urbaine du Grand Reims, Département de la Marne, Région Grand Est and European Union (FEDER Grand Est 2021–2027) are acknowledged for their financial support to the Chair of Biotechnology of CentraleSupélec and the Centre Européen de Biotechnologie et de Bioéconomie (CEBB).

Data Availability Statement: The original contributions presented in the study are included in the article, further inquiries can be directed to the corresponding author.

Conflicts of Interest: The authors declare no conflicts of interest.

References

1. International Energy Agency. 2024. Available online: <https://www.iea.org/countries/tunisia> (accessed on 20 March 2023).
2. Höök, M.; Tang, X. Depletion of fossil fuels and anthropogenic climate change—A review. *Energy Policy* **2013**, *52*, 797–809.
3. Johnsson, F.; Kjærstad, J.; Rootzén, J. The threat to climate change mitigation posed by the abundance of fossil fuels. *Clim. Policy* **2019**, *19*, 258–274.
4. IEA. Global Energy-Related Greenhouse Gas Emissions, 2000–2022. 2023. Available online: <https://www.iea.org/data-and-statistics/charts/global-energy-related-greenhouse-gas-emissions-2000-2022> (accessed on 2 March 2023).
5. Ram, M.; Child, M.; Aghahosseini, A.; Bogdanov, D.; Lohrmann, A.; Breyer, C. A comparative analysis of electricity generation costs from renewable, fossil fuel and nuclear sources in G20 countries for the period 2015–2030. *J. Clean. Prod.* **2018**, *199*, 687–704.
6. Babu, B.V. Biomass pyrolysis: A state-of-the-art review. *Biofuels Bioprod. Biorefin.* **2008**, *2*, 393–414.
7. IEA. Available online: <https://www.iea.org/world> (accessed on 20 March 2023).
8. Liu, W.; Liu, C.; Gogoi, P.; Deng, Y. Overview of Biomass Conversion to Electricity and Hydrogen and Recent Developments in Low-Temperature Electrochemical Approaches. *Engineering* **2020**, *6*, 1351–1363.
9. Trabelsi, A.B.H.; Ghrib, A.; Zaafour, K.; Friaa, A.; Ouerghi, A.; Naoui, S.; Belayouni, H. Hydrogen-Rich Syngas Production from Gasification and Pyrolysis of Solar Dried Sewage Sludge: Experimental and Modeling Investigations. *BioMed Res. Int.* **2017**, *2017*, 7831470. <https://doi.org/10.1155/2017/7831470>.
10. Trabelsi, A.B.H.; Zaafour, K.; Baghdadi, W.; Naoui, S.; Ouerghi, A. Second generation biofuels production from waste cooking oil via pyrolysis process. *Renew. Energy* **2018**, *126*, 888–896. <https://doi.org/10.1016/j.renene.2018.04.002>.
11. Hassen-Trabelsi, A.B.; Kraiem, T.; Naoui, S.; Belayouni, H. Pyrolysis of waste animal fats in a fixed-bed reactor: Production and characterization of bio-oil and bio-char. *J. Waste Manag.* **2014**, *34*, 210–218.
12. Aissaoui, M.H.; Trabelsi, A.B.H.; Bensidhom, G.; Ceylan, S.; Leahy, J.J.; Kwapinski, W. Sustainable Valorization of Olive Pomace Waste to Renewable Biofuels, Biomaterials and Biochemicals via Pyrolysis Process: Experimental and Numerical Investigation 2021. Available online: https://www.researchgate.net/publication/354942727_Sustainable_Valorization_of_Olive_Pomace_Waste_to_Renewable_Biofuels_Biomaterials_and_Biochemicals_Via_Pyrolysis_Process_Experimental_and_Numerical_Investigation (accessed on 20 March 2023).
13. Grioui, N.; Halouani, K.; Agblevor, F.A. Bio-oil from pyrolysis of Tunisian almond shell: Comparative study and investigation of aging effect during long storage. *Energy Sustain. Dev.* **2014**, *21*, 100–112.
14. Bensidhom, G.; Hassen-Trabelsi, A.B.; Alper, K.; Sghairoun, M.; Zaafour, K.; Trabelsi, I. Pyrolysis of Date palm waste in a fixed-bed reactor: Characterization of pyrolytic products. *Bioresour. Technol.* **2017**, *247*, 363–369.
15. Yang, Y.; Qian, X.; Alamu, S.O.; Brown, K.; Lee, S.W.; Kang, D.-H. Qualities and Quantities of Poultry Litter Biochar Characterization and Investigation. *Energies* **2024**, *17*, 2885. <https://doi.org/10.3390/en17122885>.

16. Vendra Singh, S.; Chaturvedi, S.; Dhyani, V.C.; Kasivelu, G. Pyrolysis temperature influences the characteristics of rice straw and husk biochar and sorption/desorption behaviour of their biourea composite. *Bioresour. Technol.* **2020**, *314*, 123674. <https://doi.org/10.1016/j.biortech.2020.123674>.
17. Khiari, B.; Jeguirim, M. Pyrolysis of Grape Marc from Tunisian Wine Industry: Feedstock Characterization, Thermal Degradation and Kinetic Analysis. *Energies* **2018**, *11*, 730. <https://doi.org/10.3390/en11040730>.
18. Ruiz, J.A.; Juárez, M.C.; Morales, M.P.; Muñoz, P.; Mendívil, M.A. Biomass gasification for electricity generation: Review of current technology barriers. *Renew. Sustain. Energy Rev.* **2013**, *18*, 174–183.
19. Ongen, A.; Ozcan, H.K.; Ozbas, E.E. Gasification of biomass and treatment sludge in a fixed bed gasifier. *Int. J. Hydrogen Energy* **2016**, *41*, 8146–8153.
20. Plis, P.; Wilk, R.K. Theoretical and experimental investigation of biomass gasification process in a fixed bed gasifier. *Energy* **2011**, *36*, 3838–3845.
21. Aydin, E.S.; Yucel, O.; Sadikoglu, H. Experimental study on hydrogen-rich syngas production via gasification of pine cone particles and wood pellets in a fixed bed downdraft gasifier. *Int. J. Hydrogen Energy* **2019**, *44*, 17389–17396. <https://doi.org/10.1016/j.ijhydene.2019.02.175>.
22. Khelifi, S.; Lajili, M.; Perré, P.; Pozzobon, V. A Numerical Study of Turbulent Combustion of a Lignocellulosic Gas Mixture in an Updraft Fixed Bed Reactor. *Sustainability* **2022**, *14*, 16587. <https://doi.org/10.3390/su142416587>.
23. Luo, S.; Zhou, Y.; Yi, C. Syngas production by catalytic steam gasification of municipal solid waste in fixed-bed reactor. *Energy* **2012**, *44*, 391–395.
24. Zheng, X.; Chen, C.; Ying, Z.; Wang, B. Experimental study on gasification performance of bamboo and PE from municipal solid waste in a bench-scale fixed bed reactor. *Energy Convers. Manag.* **2016**, *117*, 393–399.
25. Kruesi, M.; Jovanovic, Z.R.; dos Santos, E.C.; Yoon, H.C.; Steinfeld, A. Solar-driven steam-based gasification of sugarcane bagasse in a combined drop-tube and fixed-bed reactor—Thermodynamic, kinetic, and experimental analyses. *Biomass Bioenergy* **2013**, *52*, 173–183.
26. Whitty, K.J.; Zhang, H.R.; Eddings, E.G. Emissions from syngas combustion. *Combust. Sci. Technol.* **2008**, *180*, 1117–1136.
27. Zribi, M.; Lajili, M.; Escudero-Sanz, F.J. Hydrogen enriched syngas production via gasification of biofuels pellets/powders blended from olive mill solid wastes and pine sawdust under different water steam/nitrogen atmospheres. *Int. J. Hydrogen Energy* **2018**, *44*, 11280–11288.
28. Demirbas, A.; Arin, G. An Overview of Biomass Pyrolysis. *Energy Sources* **2002**, *24*, 471–482.
29. Kan, T.; Strezov, V.; Evans, T.J. Lignocellulosic biomass pyrolysis: A review of product properties and effects of pyrolysis parameters. *Renew. Sustain. Energy Rev.* **2016**, *57*, 1126–1140.
30. Andican, A.; Faizal, M.; Said, M.; Aprianti, N. Synthetic Gas Production from Fine Coal Gasification Using Low-Cost Catalyst. *J. Ecol. Eng.* **2022**, *23*, 64–72.
31. David, E. Evaluation of Hydrogen Yield Evolution in Gaseous Fraction and Biochar Structure Resulting from Walnut Shells Pyrolysis. *Energies* **2020**, *13*, 6359. <https://doi.org/10.3390/en13236359>.
32. Xie, Y.; Zeng, K.; Flamant, G.; Yang, H.; Liu, N.; He, X.; Yang, X.; Nzihou, A.; Chen, H. Solar pyrolysis of cotton stalk in molten salt for bio-fuel production: Review. *Energy* **2019**, *179*, 1124–1132.
33. Sedmihradská, A.; Pohořelý, M.; Jevič, P.; Skoblia, S.; Beňo, Z.; Farták, J.; Čech, B.; Hartman, M. Pyrolysis of wheat and barley straw. *Res. Agric. Eng.* **2020**, *66*, 8–17.
34. Mansouri, S.; Khiari, R.; Bendouissa, N.; Saadallah, S.; Mhenni, F.; Mauret, E. Chemical composition and pulp characterization of Tunisian vine stems. *Ind. Crop. Prod.* **2012**, *36*, 22–27.
35. Mlonka-Mędrala, A.; Evangelopoulos, P.; Sieradzka, M.; Zajemska, M.; Magdziarz, A. Pyrolysis of agricultural waste biomass towards production of gas fuel and high-quality char: Experimental and numerical investigations. *Fuel* **2021**, *296*, 120611.
36. Qian, X.; Xue, J.; Yang, Y.; Lee, S.W. Thermal Properties and Combustion-Related Problems Prediction of Agricultural Crop Residues. *Energies* **2021**, *14*, 4619. <https://doi.org/10.3390/en14154619>.
37. Kraiem, N.; Jeguirim, M.; Limousy, L.; Lajili, M.; Dorge, S.; Michelin, L.; Said, R. Impregnation of olive mill wastewater on dry biomasses: Impact on chemical properties and combustion performances. *Energy* **2014**, *78*, 479–489.
38. Lajili, M.; Guizani, C.; Sanz, F.J.E.; Jeguirim, M. Fast pyrolysis and steam gasification of pellets prepared from olive oil mill residues. *Energy* **2018**, *150*, 61–68.
39. Kraiem, N.; Lajili, M.; Limousy, L.; Said, R.; Jeguirim, M. Energy recovery from Tunisian agri-food wastes: Evaluation of combustion performance and emissions characteristics of green pellets prepared from tomato residues and grape marc. *Energy* **2016**, *107*, 409–418.
40. Limousy, L.; Jeguirim, M.; Dutournié, P.; Kraiem, N.; Lajili, M.; Said, R. Gaseous Products and particulate matter emissions of biomass residential boiler fired with spent coffee grounds pellets. *Fuel* **2016**, *107*, 323–329.
41. Ullah, F.; Zhang, L.; Ji, G.; Irfan, M.; Ma, D.; Li, A. Experimental analysis on products distribution and characterization of medical waste pyrolysis with a focus on liquid yield quantity and quality. *Sci. Total Environ.* **2022**, *829*, 154692.
42. Salem, A.M.; Dhami, H.S.; Paul, M.C. Syngas Production and Combined Heat and Power from Scottish Agricultural Waste Gasification—A Computational Study. *Sustainability* **2022**, *14*, 3745. <https://doi.org/10.3390/su14073745>.
43. Shi, K.; Yan, J.; Menéndez, J.A.; Luo, X.; Yang, G.; Chen, Y.; Lester, E.; Wu, T. Production of H₂-Rich Syngas from Lignocellulosic Biomass Using Microwave-Assisted Pyrolysis Coupled with Activated Carbon Enabled Reforming. *Front. Chem.* **2020**, *8*, 3. <https://doi.org/10.3389/fchem.2020.00003>.

44. Solar, J.; Caballero, B.M.; López-Uriónabarrenechea, A.; Acha, E.; Arias, P.L. Pyrolysis of Forestry Waste in a Screw Reactor with Four Sequential Heating Zones: Influence of Isothermal and Nonisothermal Profiles. *Ind. Eng. Chem. Res.* **2021**, *60*, 18627–18639.
45. Shehzad, A.; Bashir, M.J.K.; Horttanainen, M.; Manttari, M.; Havukainen, J.; Abbas, G. Modeling and comparative assessment of bubbling fluidized bed gasification system for syngas production—A gateway for a cleaner future in Pakistan. *Environ. Technol.* **2017**, *39*, 1841–1850. <https://doi.org/10.1080/09593330.2017.1340350>.
46. At Naw, S.M.; Sulaiman, S.A.; Yusup, S. Influence of Fuel Moisture Content and Reactor Temperature on the Calorific Value of Syngas Resulted from Gasification of Oil Palm Fronds. *Sci. World J.* **2014**, *2014*, 121908. <https://doi.org/10.1155/2014/121908>.
47. Dong, J.; Chi, Y.; Tang, Y.; Ni, M.; Nzihou, A.; Weiss-Hortala, E.; Huang, Q. Effect of Operating Parameters and Moisture Content on Municipal Solid Waste Pyrolysis and Gasification. *Energy Fuels.* **2016**, *30*, 3994–4001. <https://doi.org/10.1021/acs.energyfuels.6b00042>.
48. Chen, J.; Gao, S.; Xu, F.; Xu, W.; Yang, Y.; Kong, D.; Wang, Y.; Yao, H.; Chen, H.; Zhu, Y.; et al. Influence of moisture and feedstock form on the pyrolysis behaviors, pyrolytic gas production, and residues micro-structure evolutions of an industrial sludge from a steel production enterprise. *Energy* **2022**, *248*, 123603. <https://doi.org/10.1016/j.energy.2022.123603>.
49. Wang, Z.; Shi, S.; Huang, S.; Tang, J.; Du, T.; Cheng, X.; Huang, R.; Chen, J.-Y. Effects of water content on evaporation and combustion characteristics of water emulsified diesel spray. *Appl. Energy* **2018**, *226*, 397–407. <https://doi.org/10.1016/j.apenergy.2018.06.023>.
50. Fraia, D.S.; Uddin, M.R. Energy Recovery from Waste Paper and Deinking Sludge to Support the Demand of the Paper Industry: A Numerical Analysis. *Sustainability* **2022**, *14*, 4669. <https://doi.org/10.3390/su14084669>.
51. Puri, L.; Hu, Y.; Naterer, G. Critical review of the role of ash content and composition in biomass pyrolysis. *Front. Fuels* **2024**, *2*, 1378361. <https://doi.org/10.3389/ffuel.2024.1378361>.
52. Rafiq, M.K.; Bachmann, R.T.; Rafiq, M.T.; Shang, Z.; Joseph, S.; Long, R.L. Influence of Pyrolysis Temperature on Physico-Chemical Properties of Corn Stover (*Zea mays* L.) Biochar and Feasibility for Carbon Capture and Energy Balance. *PLoS ONE* **2016**, *11*, e0156894. <https://doi.org/10.1371/journal.pone.0156894>.
53. Kardaś, D.; Kluska, J.; Kazimierski, P. The course and effects of syngas production from beechwood and RDF in updraft reactor in the light of experimental tests and numerical calculations. *Therm. Sci. Eng. Prog.* **2018**, *8*, 136–144.
54. Samiran, N.A.; Jaafar, M.N.M.; Ng, J.-H.; Lam, S.S.; Chong, C.T. Progress in biomass gasification technique—With focus on Malaysian palm biomass for syngas production. *Renew. Sustain. Energy Rev.* **2016**, *62*, 1047–1062.
55. Santos, S.M.; Assis, A.C.; Gomes, L.; Nobre, C.; Brito, P. Waste Gasification Technologies: A Brief Overview. *Waste* **2023**, *1*, 140–165. <https://doi.org/10.3390/waste101001>.
56. Havilah, P.R.; Sharma, A.K.; Govindasamy, G.; Matsakas, L.; Patel, A. Biomass Gasification in Downdraft Gasifiers: A Technical Review on Production, Up-Grading and Application of Synthesis Gas. *Energies* **2022**, *15*, 3938. <https://doi.org/10.3390/en15113938>.
57. Ahmad, A.A.; Zawawi, N.A.; Kasim, F.H.; Inayat, A.; Khasri, A. Assessing the gasification performance of biomass: A review on biomass gasification process conditions, optimization, and economic evaluation. *Renew. Sustain. Energy Rev.* **2016**, *53*, 1333–1347.
58. Hu, X.; Bai, F.; Yu, C.; Yan, F. Experimental Study of the Laminar Flame Speeds of the CH₄/H₂/CO/CO₂/N₂ Mixture and Kinetic Simulation in Oxygen-Enriched Air Condition. *ACS Omega* **2020**, *5*, 33372–33379.
59. Fiore, M.; Magi, V.; Viggiano, A. Internal combustion engines powered by syngas: A review. *Appl. Energy* **2020**, *276*, 115415.
60. Gallucci, F.; Liberatore, R.; Sapegno, L.; Volponi, E.; Venturini, P.; Rispoli, F.; Paris, E.; Carnevale, M.; Colantoni, A. Influence of Oxidant Agent on Syngas Composition: Gasification of Hazelnut Shells through an Updraft Reactor. *Energies* **2020**, *13*, 102. <https://doi.org/10.3390/en13010102>.
61. Pinto, F.; André, R.; Miranda, M.; Neves, D.; Varela, F.; Santos, J. Effect of gasification agent on co-gasification of rice production wastes mixtures. *Fuel* **2016**, *180*, 407–416.
62. Dai, J.; Saayman, J.; Grace, J.R.; Ellis, N. Gasification of Woody Biomass. *Annu. Rev. Chem. Biomol. Eng.* **2015**, *6*, 77–99.
63. Lv, P.; Yuan, Z.; Wu, C.; Ma, L.; Chen, Y.; Tsubaki, N. Bio-syngas production from biomass catalytic gasification. *Energy Convers. Manag.* **2007**, *48*, 1132–1139.
64. Khezri, R.; Azlina, W.; Tan, H.B. An Experimental Investigation of Syngas Composition from Small-Scale Biomass Gasification. *Int. J. Biomass Renew.* **2016**, *5*, 6–13.
65. Katsaros, G.; Pandey, D.S.; Horvat, A.; Almansa, G.A.; Fryda, L.E.; Leahy, J.J.; Tassou, S.A. Experimental investigation of poultry litter gasification and co-gasification with beech wood in a bubbling fluidised bed reactor—Effect of equivalence ratio on process performance and tar evolution. *Fuel* **2020**, *262*, 116660.
66. Zhao, Y.; Feng, D.; Zhang, Z.; Sun, S.; Che, H.; Luan, J. Experimental Study on Autothermal Cyclone Air Gasification of Biomass. *J. Energy Resour. Technol.* **2017**, *140*, 042001.
67. Jayathilake, R.; Rudra, S. Numerical and Experimental Investigation of Equivalence Ratio (ER) and Feedstock Particle Size on Birchwood Gasification. *Energies* **2017**, *10*, 1232. <https://doi.org/10.3390/en10081232>.
68. At Naw, S.M.; Sulaiman, S.A.; Yusup, S. Syngas production from downdraft gasification of oil palm fronds. *Energy* **2013**, *61*, 491–501.
69. Skoulou, V.; Zabanitoutou, A.; Stavropoulos, G.; Sakelaropoulos, G. Syngas production from olive tree cuttings and olive kernels in a downdraft fixed-bed gasifier. *Int. J. Hydrogen Energy* **2018**, *33*, 1185–1194.

70. Peng, W.X.; Wang, L.S.; Mirzaee, M.; Ahmadi, H.; Esfahani, M.J.; Fremaux, S. Hydrogen and syngas production by catalytic biomass gasification. *Energy Convers. Manag.* **2017**, *135*, 270–273.
71. Maisano, S.; Urbani, F.; Cipiti, F.; Freni, F.; Chiodo, V. Syngas production by BFB gasification: Experimental comparison of different biomasses. *Int. J. Hydrogen Energy* **2018**, *44*, 4414–4422. <https://doi.org/10.1016/j.ijhydene.2018.11.148>.
72. Meng, F.; Meng, J.; Zhang, D. Influence of higher equivalence ratio on the biomass oxygen gasification in a pilot scale fixed bed gasifier. *J. Renew. Sustain. Energy* **2018**, *10*, 053101. <https://doi.org/10.1063/1.5040130>.
73. Yoon, S.J.; Son, Y.-I.; Kim, Y.-K.; Lee, J.-G. Gasification and power generation characteristics of rice husk and rice husk pellet using a downdraft fixed-bed gasifier. *Renew. Energy* **2012**, *42*, 163–167.
74. Zhang, S.; Feng, L.; Peng, X.; Mao, M.; Chi, Y.; Wang, F. Effect of Sludge Pellets Addition on Combustion Characteristics and Ash Behaviour of Municipal Solid Waste. *Waste Biomass Valorization* **2020**, *11*, 5351–5361. <https://doi.org/10.1007/s12649-020-00996-5>.
75. Khelifi, S.; Lajili, M.; Belghith, S.; Mezlini, S.; Tabet, F.; Jeguirim, M. Briquettes production from olive mill waste under optimal temperature and pressure conditions: Physico-chemical and mechanical characterizations. *Energies* **2020**, *13*, 1214.
76. Khardiwar, M.S.; Dubey, A.K.; Mahalle, D.M.; Kumar, S. Study on Physical and Chemical Properties of crop Residues briquettes for gasification. *Int. J. Renew. Energy Technol. Res.* **2013**, *2*, 237–248.
77. Timsina, R.; Thapa, R.K.; Moldestad, B.M.E.; Jaiswal, R.; Bhattarai, A.; Jecmenica, M.; Eikeland, M.S. Experimental evaluation of wood and grass pellets in a bubbling fluidized bed gasifier. *Energy Rep.* **2023**, *9*, 4049–4058.
78. Mikeska, M.; Najser, J.; Peer, V.; Frantík, J.; Kielar, J. Quality assessment of gas produced from different types of biomass pellets in gasification process. *Energy Explor. Exploit.* **2020**, *38*, 406–416.
79. Kurkela, E.; Kurkela, M.; Hiltunen, I. Production of Synthesis Gas from Biomass Residues by Staged Fixed-bed Gasification—Results from Pilot Test Campaigns. *Chem. Eng. Trans.* **2021**, *86*, 7–12. <https://doi.org/10.3303/CET2186002>.
80. Yasuda, H.; Murakami, T. Visualization of solid distribution with heterogeneity inside fixed bed gasifier. *J. Mater. Cycles Waste Manag.* **2020**, *22*, 1561–1568. <https://doi.org/10.1007/s10163-020-01047-w>.
81. Sharma, T.; Maya, D.M.Y.; Nascimento, F.R.M.; Shi, Y.; Ratner, A.; Lora, E.E.S.; Neto, L.J.M.; Palacios, J.C.E.; Andrade, R.V. An Experimental and Theoretical Study of the Gasification of Miscanthus Briquettes in a Double-Stage Downdraft Gasifier: Syngas, Tar, and Biochar Characterization. *Energies* **2018**, *11*, 3225. <https://doi.org/10.3390/en11113225>.
82. Arjhar, W.; Hinsui, T.; Liplap, P.; Raghavan, G.S.V. Evaluation of an Energy Production System from Sewage Sludge Using a Pilot-Scale Downdraft Gasifier. *Energy Fuels* **2013**, *27*, 229–236. <https://doi.org/10.1021/ef3012728>.
83. Singla, M.; Singh, M.; Dogra, R. Experimental investigation of imbert downdraft gasifier using rice straw briquettes. *Energy Sources Part A Recover. Util. Environ. Eff.* **2020**, *1–11*. <https://doi.org/10.1080/15567036.2020.1771478>.
84. Dogru, M. Experimental Results of Olive Pits Gasification in a Fixed Bed downdraft Gasifier System. *Int. J. Green Energy* **2013**, *10*, 348–361. <https://doi.org/10.1080/15435075.2012.655351>.
85. Raj, R.; Singh, D.K.; Tirkey, J.V. Gasifier-engine performance analysis using Co-gasification of mahua wood waste and sawdust briquette blend: An experimental and optimization approach. *Biomass Convers. Biorefin.* **2023**, *1–24*. <https://doi.org/10.1007/s13399-023-04285-8>.
86. Rasmussena, N.B.K.; Aryal, N. Syngas production using straw pellet gasification in fluidized bed allothermal reactor under different temperature conditions. *Fuel* **2019**, *263*, 116706. <https://doi.org/10.1016/j.fuel.2019.116706>.
87. Wiyono, A.; Saw, L.H.; Anggrainy, R.; Husen, A.S.; Purnawan; Rohendi, D.; Gandidi, I.M.; Adanta, D.; Pambudi, N.A. Enhancement of syngas production via co-gasification and renewable densified fuels (RDF) in an open-top downdraft gasifier: Case study of Indonesian waste. *Case Stud. Therm. Eng.* **2021**, *27*, 101205.
88. Schweitzer, D.; Gredinger, A.; Schmid, M.; Waizmann, G.; Beirow, M.; Sporn, R.; Scheffknecht, G. Steam gasification of wood pellets, sewage sludge and manure: Gasification performance and concentration of impurities. *Biomass Bioenergy* **2017**, *111*, 308–319. <https://doi.org/10.1016/j.biombioe.2017.02.002>.
89. Nobre, C.; Longo, A.; Vilarinho, C.; Gonçalves, M. Gasification of pellets produced from blends of biomass wastes and refuse derived fuel chars. *Renew. Energy* **2020**, *154*, 1294–1303.
90. Sulaiman, S.A.; Razali, N.H.M.; Konda, R.E.; At Naw, S.M.; Moni, M.N.Z. On the Diversification of Feedstock in Gasification of oil Palm Fronds. *J. Mech. Eng. Sci.* **2014**, *6*, 907–915.

Disclaimer/Publisher’s Note: The statements, opinions and data contained in all publications are solely those of the individual author(s) and contributor(s) and not of MDPI and/or the editor(s). MDPI and/or the editor(s) disclaim responsibility for any injury to people or property resulting from any ideas, methods, instructions or products referred to in the content.